Crustal Tomography of 2015 Gorkha Earthquake Source Region in Central Nepal

○Chintan TIMSINA, James MORI, Masumi YAMADA

The 2015 M_W 7.8 Gorkha earthquake caused severe damage in central Nepal. The earthquake initiated ~80 km west of Kathmandu and propagated unidirectionally toward the east along the down-dip portion of Main Himalayan Thrust (MHT). Several major aftershocks followed this event, including an M_W 7.3 near the eastern edge of the mainshock rupture. Previous geophysical studies in central Nepal have suggested significant lateral variation on the crustal structure. We image physical heterogeneities in terms of velocity and attenuation of the seismic wave using local earthquake tomography in central Nepal. In this study, we present 3D Vp and Vp/Vs models along with Qp and Qs models and their role in controlling the rupture of the Gorkha earthquake.

We used data from 42 broadband and short-period stations of a temporary aftershock monitoring network[1] which was in operation for about 11 months from June 2015 to May 2016. We selected ~2100 events from an automatic catalog[2] and manually picked the arrivals. We accepted 1854 events with an azimuthal gap <240° and at least 10 P- and 6 S-phase observations. The selected events provided ~42,000 P- and ~29,000 S- arrivals covering the entire aftershocks zone.

For the seismic velocity tomography, we followed a gradational inversion approach starting with an estimation of a 1D velocity model, followed by a 2D model, a coarse 3D model, and finally, a fine 3D model. This strategy allows us to have a reasonable smooth model even in areas with sparse ray coverage. For the 1D model, we used the events with an azimuthal gap <180° for a simultaneous inversion of hypocenters, P-wave velocity (Vp), S-wave velocity (Vs), and station corrections using VELEST[3]. For 2D and 3D, we used the iterative damped least-squares algorithm, SIMUL2000[4], for simultaneous inversion of hypocenter parameters and Vp and Vp/Vs models using absolute P and S – P times. Damping parameters were selected empirically based on the trade-off between data misfits and model variances.

For attenuation tomography, we used P- and S-wave spectra. First, we modeled the amplitude spectra for the path-averaged, frequency-independent attenuation operator (t*) using a non-linear least square technique by assuming a ω^{-2} source model for the frequency band of 1-30 Hz. This procedure depends on finding an optimal fit between observed spectra and theoretically computed spectra based on the low-frequency spectral level (Ω_o), corner frequency (f_c), and t*. We obtained ~17,000 t* observations for P and ~19,000 t* observations for S, which are then inverted for attenuation structure in terms of quality factor (Qp and Qs) models using SIMUL2000 code[4]. We used the 3D velocity models and hypocenter locations from our previous velocity tomography of the region for the ray tracing.

We performed several resolution tests to identify the area of adequate resolution in our 3D models. First, we use our final inversion's full model resolution matrix to calculate the spread function (SF)[5]. We also inspect the size and direction of lateral smearing by contours where the resolution is 70% of the diagonal elements of the node. In general, small SF values indicate a high resolution of the node. As another resolution test, we performed the checkerboard

resolution test (CRT) by designing a synthetic velocity model having alternating fast and slow values with a magnitude of 5% changes relative to the 1D model. We then calculated synthetic travel times using our actual data's source-receiver configuration. We added Gaussian noise to the calculated travel times and finally inverted to see how well the original model is recovered. Additionally, we carried out the restoring resolution tests by designing a synthetic velocity model with key features observed in our final 3D models. Synthetic travel times with additional Gaussian noise were calculated as in the CRT. We repeated the entire inversion workflow starting with 1D model with the same control parameters of our real inversion. Results of these resolution assessments show that inversion is robust in the central part of the area to the depth of 15 km.

Results of our velocity and attenuation models are consistent with broad geological features and previous geophysical studies of the region. An east-west elongated low Vp zone in the southern part of the area at shallow depth (<10 km) is spatially well-correlated with sedimentary rocks of the sub-Himalaya. Since our inversion technique linearly interpolates velocities between nodes, the exact northern boundary of this low-velocity zone cannot be well represented with our relative course inversion nodes. In the central-northern part of the area, at depths 0 to 5 km, a zone of low Vp/Vs ratio (<1.65) is found. Previous studies also report such a low Vp/Vs ratio at shallow crustal depth in another segment of the Himalaya[6]. This anomalous low ratio may represent bodies of felsic (quartz-rich) rocks as mapped at the surface.

Our results from the velocity inversion at 10 km depth show the area of large (>4 m) co-seismic slip of Gorkha earthquake mainshock generally coincides with the region of high Vp and high Qp. This high velocity and low attenuation zone may represent an asperity on the fault, which possibly controlled the mainshock rupture.

References

1. Karplus et. al., 2020, Seismol. Res. Lett. 91 (4): 2399–2408

2. Yamada et. al., 2019, Bull. Seismol. Soc. Am. 110, 26–37

3. Kissling et.al., 1994, J. Geophys. Res.99, 19635–19646

4. Thurber and Eberhart-Phillips, 1999, Comput. Geosci., 25, 809–818

5. Michelini and McEvilly, 1991, Bull. Seismol. Soc. Am. 81, 524–552
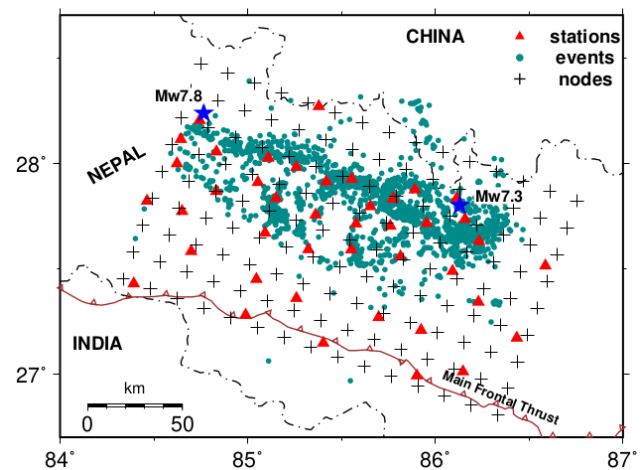
6. Monsalve et. al., 2008, J. Geophys. Res. 113

Figure 1: Distribution of events and stations used in this study.